Density profile in shock wave fronts of partially ionized xenon plasmas

2003 J. Phys. A: Math. Gen. 36 5991

(http://iopscience.iop.org/0305-4470/36/22/321)

INSTITUTE OF PHYSICS PUBLISHING JOURNAL OF PHYSICS A: MATHEMATICAL AND GENERAL

J. Phys. A: Math. Gen. **36** (2003) 5991–5997 PII: S0305-4470(03)55128-9

Density profile in shock wave fronts of partially ionized xenon plasmas

H Reinholz[1,2], G Röpke[2], I Morozov[3], V Mintsev[4], Yu Zaparoghets[4], V Fortov[4] and A Wierling[2,5]

[1] School of Physics, UWA, 35 Stirling Highway, Crawley, WA 6009, Australia
[2] Fachbereich Physik, Universität Rostock, 18051 Rostock, Germany
[3] Institute of High Energy Densities, IVTAN, Moscow, Russia
[4] Institute of Problems of Chemical Physics, Chernogolovka, Russia
[5] Department of Fundamental Energy Science, Kyoto University, Japan

E-mail: heidi@physics.uwa.edu.au

Received 21 October 2002, in final form 18 December 2002
Published 22 May 2003
Online at stacks.iop.org/JPhysA/36/5991

Abstract

Results for the reflection coefficient of shock-compressed dense xenon plasmas at pressures of 1.6–20 GPa and temperatures around 30 000 K are interpreted. In addition to former experiments using laser beams with $\lambda = 1.06$ μm, measurements at $\lambda = 0.694$ μm have been performed recently. Reflectivities typical for metallic systems are found at high densities. Besides free carriers, the theoretical description also takes into account the influence of the neutral component of the plasma on the reflectivity. A consistent description of the measured reflectivities is achieved only if a finite width of the shock wave front is considered.

PACS numbers: 52.25.Mq, 52.27.Gr, 52.38.Dx

1. Introduction

The measurement of the optical reflectivity on dense plasmas is an important diagnostic tool. In particular, it is expected that information about thermodynamic parameters, such as the free charge carrier density, can be deduced. For instance, measurements on shock-compressed aluminium and silicon are reported by Basko *et al* [1], and the change of the free electron density and the temperature across the shock wave front has been investigated.

Of particular interest are reflectivity measurements on material in which a transition from a dielectric to a metal-like behaviour occurs with increasing density due to pressure ionization. Recent measurements on hydrogen and deuterium [2] have shown such a transition which is indicated by a strong increase of the reflectivity up to metallic-like values. It is an interesting issue whether pressure ionization can be observed in other dielectrics such as rare gases.

Reflectivity measurements in dense xenon plasmas, which were produced by intense shock waves, have been performed with a laser beam of the wavelength $\lambda_1 = 1.06\ \mu$m [3]. Recently, measurements at a second wavelength of $\lambda_2 = 0.694\ \mu$m [4] using the same experimental set-up have become available. At pressures in the region of 1.6–20 GPa and temperatures around 30 000 K a strong increase of the reflectivity was observed.

In this paper, we will focus on the theoretical analysis of these results within a quantum statistical approach to the dielectric function using linear response theory. In addition to an earlier work [5], particular focus will be on the role of the neutral component in the partially ionized plasma. Furthermore, the density profile of the shock wave front, based on measurements of the reflectivity at different wavelengths, will be investigated.

2. Reflectivity measurements

In [3], an experimental set-up has been described to generate dense xenon plasmas by using explosively driven shock waves. A detonation accelerates a metal impactor up to velocities of 5–6 km s^{-1}. The impactor runs into the bottom of the experimental vessel which is filled with xenon at an initial pressure of 2–5.7 MPa and produces an intense shock wave in the gas. Compression and irreversible heating produce a dense plasma. Reflectivity was then measured using pulsed probe lasers of wavelengths $\lambda_1 = 1.06\ \mu$m [3] and $\lambda_2 = 0.694\ \mu$m [4].

In order to control the spatial and temporal plasma slug parameters, the optical image of the shock wave in xenon was recorded by a PCO camera. The impactor velocity was measured with the electro-contact basis method. The thermodynamic parameters of the plasma were determined from the measured shock wave velocity. The plasma composition was calculated within a chemical picture [6]. Working with a grand canonical ensemble [7], virial corrections have been taken into account due to charge–charge interactions (Debye approximation). Short-range repulsion of heavy particles was considered within the framework of a soft sphere model. In the parameter range of the shock wave experiments, derivations of up to 20% for the composition have been obtained depending on the approximations for the equation of state. This is within the accuracy of the experimental values of the reflectivity.

The intensity of the probe radiation was about 10^4 W cm^{-2}. The registration of the radiation, reflected from the xenon plasma, was carried out by broadband photodetectors. The plasma reflection coefficient was determined from the ratio of the photodetector signal, which recorded the reflected radiation, and the photodetector signal, which fixed the probe impulse. The accuracy of the measured values of the reflection coefficient is better than 10%. For further details of the experimental set-up refer to [3]. Recently, the measurements have been repeated at a different laser wavelength [4], but using the same experimental set-up.

Experimental results [3, 4] for the reflectivity R are shown in tables 1 and 2 along with the thermodynamic parameters pressure P, temperature T, mass density ρ, free electron number density n_e, density of neutral atoms n_a, ionization degree $\alpha_{\rm ion} = n_e/(n_e + n_a)$ as well as the non-ideality parameter $\Gamma = e^2\beta(4\pi n_e/3)^{1/3}/(4\pi\epsilon_0)$ and the degeneracy parameter $\Theta = 1/(\beta E_F)$. Note that E_F is the Fermi energy and $\beta = 1/k_{\rm B}T$. The pulsed probe lasers of wavelengths $\lambda_1 = 1.06\ \mu$m [3] and $\lambda_2 = 0.694\ \mu$m [4] relate to a critical density $n_e^{\rm cr}$ of 1.02×10^{21} cm^{-3} and 2.35×10^{21} cm^{-3}, respectively, defined via the plasma frequency of the plasma as $\omega = \omega_{\rm pl} = \left(n_e^{\rm cr} e^2 / \epsilon_0 m_e\right)^{1/2}$.

The measured reflection coefficient shows a strong increase which indicates a transition from a dielectric to a metal-like behaviour. Assuming local equilibrium and plasma parameters as given in tables 1 and 2, we examine whether the observed reflectivities can be reproduced from theoretical approaches to the plasma properties.

Table 1. $\lambda_1 = 1.06\ \mu$m [3].

P (GPa)	$R^{\exp}$	T (K)	ρ (g cm^{-3})	n_e (cm^{-3})	n_a (cm^{-3})	$\alpha_{\rm ion}$	Γ	Θ
1.6	0.096	30 050	0.51	1.8×10^{21}	6.1×10^{20}	0.75	1.1	4.8
3.1	0.12	29 570	0.97	3.2×10^{21}	1.4×10^{21}	0.70	1.3	3.2
5.1	0.18	30 260	1.46	4.5×10^{21}	2.2×10^{21}	0.67	1.5	2.6
7.3	0.26	29 810	1.98	5.7×10^{21}	3.5×10^{21}	0.62	1.6	2.2
10.5	0.36	29 250	2.70	7.1×10^{21}	5.4×10^{21}	0.57	1.8	1.9
16.7	0.47	28 810	3.84	9.1×10^{21}	8.6×10^{21}	0.51	2.0	1.6

Table 2. $\lambda_2 = 0.694\ \mu$m [4].

P (GPa)	$R^{\exp}$	T (K)	ρ (g cm^{-3})	n_e (cm^{-3})	n_a (cm^{-3})	$\alpha_{\rm ion}$	Γ	Θ
4.1	0.11	33 000	1.1	3.8×10^{21}	1.3×10^{21}	0.75	1.3	3.2
9.1	0.18	32 000	2.2	6.6×10^{21}	3.6×10^{21}	0.65	1.6	2.1
20.0	0.43	29 000	4.1	8.8×10^{21}	9.9×10^{21}	0.47	1.9	1.6

3. Step-like plasma front

Assuming a step-like plasma front [8] and normal incidence, the reflection coefficient $R(\omega)$ is related to the dielectric function $\epsilon(\omega)$ according to the Fresnel formula

$$R(\omega) = \left| \frac{\sqrt{\epsilon(\omega)} - 1}{\sqrt{\epsilon(\omega)} + 1} \right|^2 . \tag{1}$$

Via a generalized Drude formula [5, 9, 10]

$$\epsilon(\omega) = 1 - \frac{\omega_{\rm pl}^2}{\omega[\omega + {\rm i}\nu(\omega)]} \tag{2}$$

the dynamical collision frequency $\nu(\omega)$ is introduced. In this way, the calculation of the reflectivity is traced back to the evaluation of the dynamical collision frequency.

Using linear response theory [9, 11], the dynamical collision frequency can be represented by force–force correlation functions in thermal equilibrium. According to the decomposition of the force into electron–ion and electron–atom interaction, the collision frequency is given as $\nu(\omega) = \nu_{ei}(\omega) + \nu_{ea}(\omega)$ in a partially ionized plasma. We first consider the contribution $\nu_{ei}(\omega)$ due to electron–ion collisions. It can be evaluated using different methods such as quantum MD simulations or perturbative expansions of thermodynamic Green functions.

The details of the evaluation of $\nu_{ei}(\omega)$ using the method of thermodynamic Green functions are given in [9]. In that context, different approximations for the collision frequency have been derived with respect to a systematic perturbation theory [5]. The singular behaviour of the unscreened Born approximation $\left(\nu_{ei}^{\rm Born}(\omega)\right)$ is removed if screening of the interaction potential (interaction at long distances, Lennard–Balescu collision term $\nu_{ei}^{\rm LB}(\omega)$) as well as the T matrix term $\left(\nu_{ei}^{\rm T}(\omega)\right)$ describing strong collisions at short distances is considered. To avoid double counting, the following combination has been proposed by Gould and deWitt [12]:

$$\nu_{ei}^{\rm GD}(\omega) = \nu_{ei}^{\rm T}(\omega) - \nu_{ei}^{\rm Born}(\omega) + \nu_{ei}^{\rm LB}(\omega). \tag{3}$$

Furthermore, a renormalization factor $r(\omega)$, entering via the generalized Drude formula (2) as $\nu_{ei}(\omega) \approx r(\omega)\nu_{ei}^{\rm GD}(\omega)$, follows from taking into account higher moments of single-particle distribution functions as well as including effects of electron–electron collisions, see [9].

Table 3. Reflectivities for $\lambda_1 = 1.06\ \mu$m from step-like density profile.

P (GPa)	R^{exp}	$R_{\mathrm{dc}}^{\mathrm{ERR}}$	$R_{\mathrm{dc}}^{\mathrm{ERR,ea}}$	$R_{\mathrm{dc}}^{\mathrm{ERR,ea,b}}$	R^{MD}
1.6	0.096	0.502	0.464	0.452	0.044
3.1	0.12	0.588	0.543	0.531	0.100
5.1	0.18	0.630	0.585	0.572	0.136
7.3	0.26	0.661	0.609	0.593	0.166
10.5	0.36	0.692	0.635	0.616	0.200
16.7	0.47	0.729	0.668	0.646	0.233

Based on this systematic approach to the collision frequency, an interpolation formula [13] for the static collision frequency $\nu_{ei}(\omega = 0) \approx \nu_{ei,\mathrm{dc}}^{\mathrm{ERR}}$ was derived. It corresponds to a static conductivity and has been used to evaluate the reflectivity of a step-like plasma front as presented in table 3. The calculated reflectivities are too high in comparison to the experimental values. Improvements in the theoretical description due to a frequency dependence of the collision frequency [5] show only a minor effect at the parameter values of the experiments.

4. Partially ionized plasma

As can be seen from the thermodynamic parameters in tables 1 and 2, the fraction of neutral particles in the plasma is not negligible. The plasma is in fact a partially ionized system and contributions resulting from the additional scattering mechanism of electrons with atoms as well as a direct contribution of the neutral component to the dielectric function, which was neglected in former work [5], will be discussed here.

The scattering of the electrons on the atoms can be described by a screened polarization potential [14]

$$V_{\mathrm{p}}(r) = \frac{e^2}{4\pi\epsilon_0}\frac{\alpha_{\mathrm{p}}}{2\left(r^2 + r_0^2\right)^2}\,\mathrm{e}^{-2\kappa r}(1+\kappa r)^2 \qquad \text{with} \quad \kappa^2 = 2n_e\beta\frac{e^2}{\epsilon_0} \tag{4}$$

and the polarizability $\alpha_{\mathrm{p}} = 27.3a_{\mathrm{B}}^3$ [15] for xenon. The cut-off parameter r_0 ensures the finite size of the polarization potential at small distances $r \to 0$ from the atom. It is caused by the finite extension of the atomic charge distribution so that the $1/r^4$ dependence valid for the unscreened electron–atom interaction at large distances is modified at short distances. The cut-off parameter was chosen to be the atomic radius [15] $r_0 = 1\ \text{Å} = 1.89a_{\mathrm{B}}$. Another commonly used option is given by the formula $r_0^4 = \alpha_{\mathrm{p}}Z^{-1/3}a_{\mathrm{B}}/2$ [16] which leads to $r_0 = 1.49a_{\mathrm{B}}$. However, this value is inconsistent in the case of xenon because the polarization potential would appear to be stronger than the Coulomb potential of the ion at distances around $r = 1a_{\mathrm{B}}$.

Evaluating the force–force correlation function, the electron–atom interaction leads to an additional contribution to the collision frequency $\nu_{ea}(\omega)$. In static Born approximation, the respective collision frequency is [14]

$$\nu_{ea,\mathrm{dc}} = n_a\frac{e^4\beta^{3/2}}{6\sqrt{2}\pi^{3/2}\epsilon_0^2 m_e^{1/2}}\left(\frac{m_e\pi\alpha_{\mathrm{p}}}{\beta\hbar^2 r_0}\right)^2\frac{1}{2}\int_0^\infty \mathrm{d}y\,\frac{y^5}{(y+\kappa^2 l^2)^4}\,\mathrm{e}^{-y-2\frac{r_0}{l}\sqrt{y}} \tag{5}$$

where $l^2 = \frac{\beta\hbar^2}{8m_e}$. The strength of the scattering could be directly compared with the electron–ion scattering by omitting the factors of the particle density in the collision frequencies. The ratio $\nu_{ea,\mathrm{dc}}n_e\big/\left(\nu_{ei,\mathrm{dc}}^{\mathrm{ERR}}n_a\right)$ is about one third.

The neutral component of the partially ionized plasma also gives an additional direct contribution to the dielectric function. According to a cluster expansion of the polarization function [17], several terms can be discussed. The main contribution comes from transitions bound-continuum and can be approximated by

$$\epsilon_{ea}(\omega) = 4\pi\alpha_{\mathrm{p}} n_a \frac{1}{1-(\hbar\omega/E_{1s})^2}. \tag{6}$$

Table 3 shows the reflectivities $R_{\mathrm{dc}}^{\mathrm{ERR}}$ calculated from the fit formula for the collision frequency $\nu_{ei,\mathrm{dc}}^{\mathrm{ERR}}$. $R_{\mathrm{dc}}^{\mathrm{ERR,ea}}$ takes into account the additional contribution (5) in the collision frequency. Furthermore, in $R_{\mathrm{dc}}^{\mathrm{ERR,ea,b}}$, the atomic contribution to the dielectric function (6) has been added. The atomic contributions lead to a reduction of the reflectivity by about 10%. The experimental values R^{exp} and results from quasi-classical Monte Carlo simulations R^{MD} [18] are given as well. In comparison with the perturbative treatment, the Monte Carlo simulations lead to lower reflectivity values. This may be related to the use of a quasi-classical pseudopotential as proposed by Deutsch. In both cases, the steep increase of the reflectivity with density as seen in the experiments cannot be explained satisfactorily.

5. Finite shock front width

Based on the assumption of local thermal equilibrium, it has been shown that it is not possible to interpret the measured values of the reflection coefficient of dense xenon plasmas within the assumption of a step-like density profile, i.e. $d \approx 0$ for width of the shock wave front. In particular, the steep increase of the reflectivity only at densities above the critical one cannot be explained despite a highly sophisticated approach to the calculation of the dielectric function.

If a density profile of the shock wave front is considered assuming the free electron density increases smoothly from zero to its maximum value n_e above n_e^{cr}, the reflection of electromagnetic radiation occurs already in the outer region where the density is low. Within a simplified picture, the radiation penetrates the low-density region of the plasma up to the region where the density approaches the critical value. Here the wave is reflected.

The reflectivity from an arbitrary plasma front can be obtained from the direct solution of the equation for electromagnetic fields. Let us consider a planar wave propagating along the z-axis. Neglecting non-local effects for the conductivity we write the following Helmholtz equation [19] for the complex amplitude of the electric field with frequency ω:

$$\frac{\mathrm{d}^2 E(z)}{\mathrm{d}z^2} + 2\pi\epsilon(\omega, z)E(z) = 0 \tag{7}$$

where $z = d/\lambda$ is the distance in units of the laser wavelength. The dielectric function $\epsilon(\omega, z)$ can be calculated from (2) for given density and temperature profiles $n_e(z)$, $T(z)$ according to $\nu_{ei,\mathrm{dc}}^{\mathrm{ERR}}(n_e, T)$, which in principle can be improved accounting for frequency dependence, contribution of neutral bound states, etc.

The appropriate solution of (7) is selected by taking the boundary condition

$$E(z_0) = E_0 \exp\{-2\pi \mathrm{i} z_0 \sqrt{\epsilon(\omega, z_0)}\} \qquad E'(z_0) = -2\pi \mathrm{i}\sqrt{\epsilon_0(\omega, z_0)}E(z_0). \tag{8}$$

Then, equation (7) is solved numerically, starting from the initial point z_0. The reflectivity is given by [19]

$$R = \frac{|E_r(z_1)|^2}{|E_i(z_1)|^2} \tag{9}$$

where

$$E_i(z) = \frac{1}{2}\left(E(z) - \frac{E'(z)}{2\pi\mathrm{i}}\right) \qquad \text{and} \qquad E_r(z) = \frac{1}{2}\left(E(z) + \frac{E'(z)}{2\pi\mathrm{i}}\right) \tag{10}$$

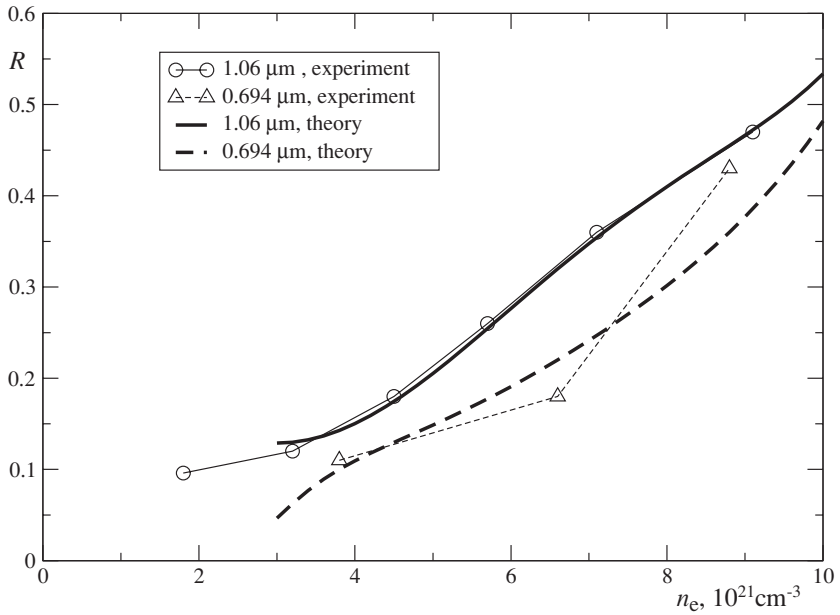

Figure 1. Reflectivity coefficient for xenon assuming profile with two Fermi-like decays (11) (theory) compared with experimental results.

describe incident and reflected waves correspondingly and z_1 is taken to be in the free space region ($\epsilon(\omega, z_1) = 1$).

Smooth density profiles for a shock wave front such as a linear decrease or a spatial variation according to a Fermi function have been considered and parameters were fitted to reproduce the experimental values of the reflectivity. By using measurements of the reflectivity at different wavelengths it is possible to determine more details of the density profile and find a consistent description of $R(\omega)$. In the following, a density profile with two Fermi-like decays is assumed:

$$n_e(z) = [n_e - n_0(n_e)]\frac{1}{e^{z/l_1(n_e)} + 1} + n_0(n_e)\frac{1}{e^{z/l_2(n_e)} + 1}. \tag{11}$$

Reasonable parameter values to fit all experimental data given above are $n_0(n_e) = 0.055n_e^2 + 0.34n_e - 0.014$, $l_1(n_e) = 0.01n_e^2 - 0.18n_e + 1.1$ μm and $l_2(n_e) = -0.0033n_e^2 + 0.041n_e - 0.024$ μm, and the densities have to be taken in units of 10^{21} cm^{-3}. The comparison between this broad range fit to the density profile and the measured results is shown in figure 1.

6. Conclusions

Linear response theory for the dielectric function $\epsilon(k, \omega)$ which is applicable in the entire $\vec{k}, \omega$-plane allows for a perturbative treatment. A generalized Drude formula [5, 9, 10] was applied for the calculation of the reflectivity. The influence of bound states and a cluster expansion of the dielectric function in order to take into account atomic contributions have been considered. However, only minor corrections have been obtained in the reflectivity. The relevance of a finite density profile in the shock wave front in order to explain the sharp increase of reflectivity has been argued. The application of MD simulations has been reported; for details see a contribution within this volume [18]. The density profiles should be obtained from

hydrodynamic calculations with ionization reactions, which is a slow process compared with the thermal equilibration due to collisions. Experimental investigations at further frequencies would be desirable.

Acknowledgments

We acknowledge support from the DFG within the SPP 1053 'Wechselwirkung intensiver Laserfelder mit Materie' and the SFB 198 'Kinetik partiell ionisierter Plasmen' as well as via the grant RFBR-DFG no 99-02-04018. IM acknowledges grant RFBR no 00-02-16310 and 01-02-06382, and HR acknowledges a DFG research fellowship.

References

[1] Löwer T, Kondrashov V N, Basko M, Kendl A, Meyer-ter-Vehn J, Sigel R and Ng A 1998 *Phys. Rev. Lett.* **80** 4000
Basko M, Löwer T, Kondrashov V N, Kendl A, Sigel R and Meyer-ter-Vehn J 1997 *Phys. Rev.* E **56** 1019
[2] Celliers P M *et al* 2000 *Phys. Rev Lett.* **84** 5564
Cauble R *et al* 2001 *Contrib. Plasma Phys.* **41** 239
[3] Mintsev V B and Zaporoghets Yu B 1989 *Contrib. Plasma Phys.* **29** 493
[4] Zaporoghets Yu B, Mintsev V B, Gryaznov V K and Fortov V E 2002 *Physics of Extreme States of Matter* eds V E Fortov *et al* (Chernogolovka) p 188 (in Russian)
[5] Reinholz H, Röpke G, Wierling A, Mintsev V and Gryaznov V 2003 *Contrib. Plasma Phys.* **43** 3
[6] Ebeling W 1969 *Physica* **43** 293
Ebeling W, Förster A, Fortov V, Gryaznov V K and Polishchuk A 1991 *Thermophysical Properties of Hot Dense Plasmas* (Stuttgart: Teubner)
[7] Fortov V E, Gryaznov V K, Mintsev V B, Ternovoi V Ya, Iosilevski I L, Zhernokletov M V and Mochalov M A 2001 *Contrib. Plasma Phys.* **41** 215
[8] Rozmus W, Tikhonchuk V T and Cauble R 1996 *Phys. Plasmas* **3** 360
[9] Reinholz H, Redmer R, Röpke G and Wierling A 2000 *Phys. Rev.* E **62** 5648
[10] Selchow A, Reinholz H, Röpke G, Wierling A, Pschiwul T and Zwicknagel G 2001 *Phys. Rev.* E **64** 056410
[11] Zubarev D N, Morozov V and Röpke G 1997 *Statistical Mechanics of Nonequilibrium Processes* (Berlin: Akademie Verlag/Wiley)
[12] Gould H A and DeWitt H E 1967 *Phys. Rev.* A **25** 1623
[13] Esser A, Redmer R and Röpke G 2003 *Contrib. Plasma Phys.* **43** 33
[14] Redmer R 1997 *Phys. Rev.* **282** 35
[15] Fraga S, Karwowski J and Saxena K M S 1976 *Handbook of Atomic Data* (Amsterdam: Elsevier)
[16] Mittleman M H and Watson K M 1959 *Phys. Rev.* **113** 198
[17] Kraeft W-D, Kremp D, Ebeling W and Röpke G 1986 *Quantum Statistics of Charged Particle System* (New YorkBerlin: Plenum/Akademie Verlag)
[18] Morozov I, Norman G, Valuev A A and Valuev I A 2003 *J. Phys. A: Math. Gen.* **36** 6005–12
[19] Lekner J 1987 *Theory of Reflection* (Dordrecht: Martinus Nijhoff)